scientific reports

Check for updates

OPEN

A predictive model for diagnosing peripheral pulmonary lesions using radial probe endobronchial ultrasound images

Minlong Zhang[1,2]✉, Cuiping Yang[1,2] & Yinghua Guo[1]✉

Radial probe endobronchial ultrasound transbronchial lung biopsy with guide sheath (RP-EBUS-GS-TBLB) was one of the main diagnostic methods for peripheral pulmonary lesions (PPLs). The aim of this study was to develop a predictive model for the diagnostic rate of RP-EBUS-TBLB in PPLs. A total of 189 consecutive patients with PPLs who had undergone RP-EBUS-TBLB between January 2022 and October 2024 in 8th Medical Centre, Chinese PLA General Hospital were enrolled in this retrospective single-center cohort study. The LASSO regression method was used to select predictors and nomogram model was developed using multivariate logistic regression. Internal validation was performed using bootstrapping. Model performance was evaluated using the area under the curve (AUC), calibration curves, and decision curve analysis (DCA). Bootstrapping method was applied for internal validation. The diagnostic rate of RP-EBUS-TBLB in PPLs was 74.07% (140/189). Six (lesion morphology in CT, number of biopsies, size, margin, echogenicity and RP-EBUS location) variables were selected by the LASSO regression analysis. We applied EBUS imaging features (size, margin, echogenicity and RP-EBUS location; model 1) separately and combined them with clinical features (lesion morphology in CT and number of Biopsies; model 2) to develop two predictive models. The AUC of model 1 was 0.889 (95% CI, 0.826–0.943), and it was 0.917 (95% CI, 0.862–0.960) in model 2. The predictive model was well calibrated and DCA indicated its potential clinical usefulness. However, there is no significant difference in AUC between the two models, which suggest that the model 1(only using EBUS imaging features) can serve as a concise and efficient predictive model and has great potential to predict the diagnostic rate of RP-EBUS-TBLB in PPLs.

Keywords Endobronchial ultrasound, Guide-sheath, Peripheral pulmonary lesions, Predictive model, Diagnosis

With the popularization of chest computed tomography (CT), the incidence of peripheral pulmonary lesions (PPLs) that require early diagnosis has increased significantly[1,2]. Radial probe endobronchial ultrasound (RP-EBUS) uses a rotating transducer that can be inserted with or without a guide sheath (GS) through the bronchoscope's working channel. RP-EBUS produces a 360° image of the surrounding structures and allows the realtime detection of a lesion. Radial probe endobronchial ultrasound transbronchial lung biopsy with guide sheath (RP-EBUS-GS-TBLB) has been performed in the assessment of PPLs[3–5]. It has been reported that the overall diagnostic yield of RP-EBUS-GS was 81% and 69% for malignant and benign lesions, respectively[6–9]. RP-EBUS-TBLB is widely used for the diagnosis of PPLs, this study analyzed the clinical observation indicators of the diagnostic rate with RP-EBUS-TBLB, established and compared two risk prediction model, and improved the the diagnostic rate of PPLs with RP-EBUS-TBLB.

[1]College of Pulmonaryand Critical Care Medicine, 8th Medical Centre, Chinese PLA General Hospital, No.17 Heishanhu Rd, Haidian District, Beijing 100091, People's Republic of China. [2]Minlong Zhang and Cuiping Yang have contributed equally to this work. ✉email: 740720039@qq.com; 15991798305@163.com

Methods

Data source

This retrospective single-center study was based on the clinical records of PPLs patients diagnosed through RP-EBUS-GS-TBLB retrieved from the Department of Respiratory and Critical Care Medicine of 8th Medical Centre, Chinese PLA General Hospital between January 2022 and October 2024. All procedures performed in studies involving human participants were in accordance with the ethical standards of the institutional and/or national research committee and with the 1964 Helsinki declaration and its later amendments or comparable ethical standards. The study was approved by the institutional ethics committee of the hospital (No. 202400216). Written informed consent was obtained from all participants before inclusion.

Participants

We included PPLs patients diagnosed through RP-EBUS-GS-TBLB hospitalized for diagnostic of PPLs. The exclusion criteria were as follows: (1) Patients experienced serious complications (such as severe pleural reactions(intense pain, coughing, dizziness, sweating, pallor, palpitations, dyspnea, changes in blood pressure, nausea, and even fainting, requiring immediate medical attention), pneumothorax, severe bleeding 100 ml) during bronchsocopy; (2) Patients underwent combined use of other methods (such as bronchoalveolar lavage, Endobronchial Ultrasound-guided Transbronchial Needle Aspiration-EBUS-TBNA) during bronchsocopy; (3) incomplete medical records. According to whether the PPLs successfully diagnosed (In the pathological report, if there is only bronchial mucosal tissue and normal lung tissue, and no other findings, we consider it a diagnostic failure. However, all other pathological results, whether benign or malignant, are considered diagnostic success), all patients were divided into a diagnostic success group and a diagnostic failure group. The following variables were collected from this study: patient's gender, age, smoking history, underlying lung disease (chronic obstructive pulmonary disease COPD, asthma, interstitial lung disease ILD, other disease such as old pulmonary TB); CT characters: lesion morphology (Solid lesions, ground glass GG lesions and mixed lesions), distance from pleura; surgery procedure features: lesions location, anesthesia type (general anesthesia or local anesthesia), examination time, number of Biopsies; EBUS imaging features (Fig. 1): size of lesion (long axis), margin (more than 50% of the boundary that can be well-defined on the ultrasound image belongs to distinct margin, otherwise it is indistinct), shape (regular is defined as round or oval shape, and irregular means polygonal or complex shape), echogenicity (homogeneous means the consistency of internal echo except for the internal blood vessels and air-bronchogram, otherwise as heterogeneous), RP-EBUS location (probe within the lesion or adjacent to the lesion).

Surgical technique

Patient underwent flexible bronchoscopy (BF P260F, Olympus, Japan) 4.0 mm in external diameter for complete inspection of airways before echoendoscopy. The EBUS (EU-M30S, Olympus, Japan) was integrated with a 20-MHz radial probe (UM-S30-20R, Olympus, Japan).

2.0 mm in external diameter and guide sheath suit (K-203, Olympus, Japan). A biopsy forceps or brush was inserted into guide sheath (GS) before procedure adherence to guidelines, marked the position and then fixed

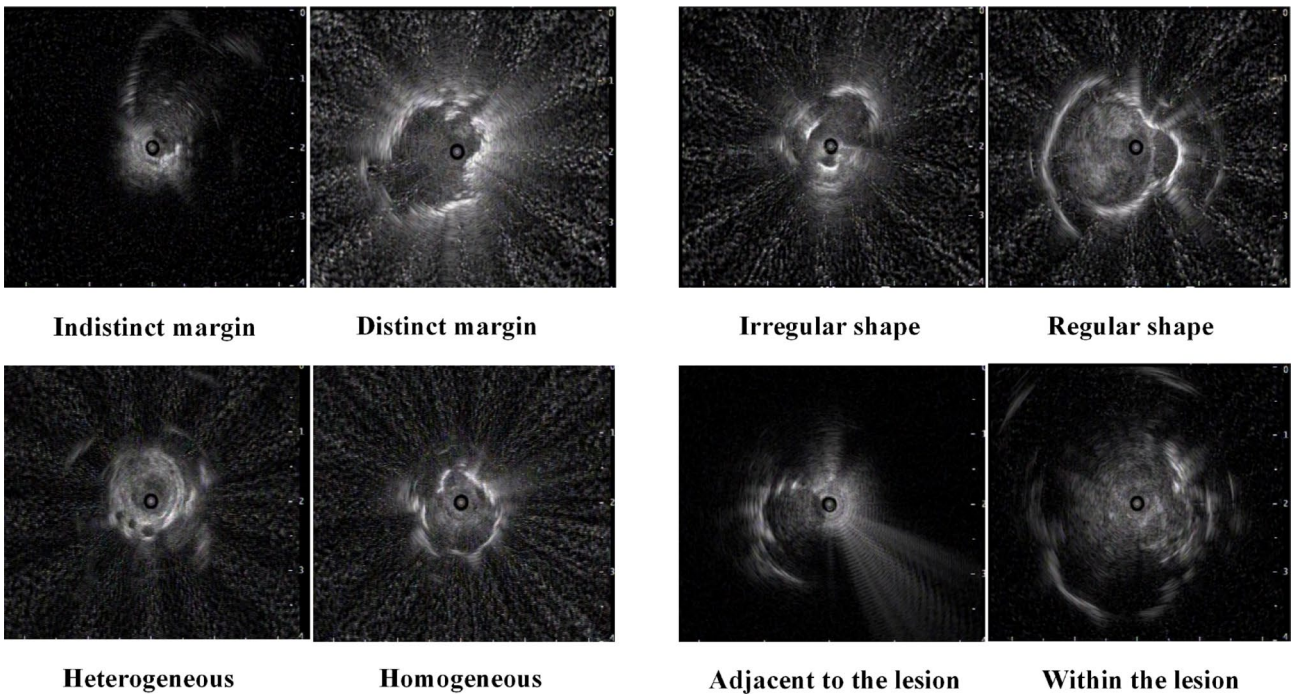

Fig. 1. Diagram of RP-EBUS grayscale features for pulmonary lesions.

probe into GS. The GS-covered probe was inserted through the work channel of the bronchoscope and advanced to the lesions to get the EBUS images. After the PPL was found, the RP was withdrawn, leaving the GS in place. Then bronchial brush (LK-NK-XBS-P, Lungcare, China) or biopsy forceps (LK-NK-IIJQ-C, Lungcare, China) were introduced into the GS, and brushings and biopsy specimens were collected (Forceps was used in all of the cases and brush was used in the vast majority of cases, and the sequence was forceps first and then brush. In a small number of cases, slight adjustments were made due to the specific circumstances at the time). Next, these specimens would undergo pathological or next-generation sequencing (NGS) testing. In addition, needle is recognized as gold standard for eccentric r-ebus lesions. in our study, we have not used needle as a diagnostic tool and we considered the following factors: First, our research focus is to explore the diagnostic effect and safety of using EBUS-GS with biopsy forceps or brush in a specific patient group. The needle is not a tool that was pre - set in our research plan. Second, from the perspective of actual operation, the use of the needle may bring some additional risks, such as complications related to puncture, bleeding, and infection. We hope to use a relatively safer and effective way to obtain samples for diagnosis. In our experience, biopsy forceps and brushes can meet most diagnostic needs. Finally, we have also conducted a detailed analysis and evaluation of the diagnostic results using biopsy forceps and brushes during the research process. The results show that in our patient sample, this method can provide sufficient diagnostic information and has achieved our research objectives.

Statistical analysis

Data were expressed as mean ± standard deviation (SD) for continuous variables, whereas categorical variables were summarized as counts (percentage). Between two groups comparison, unpaired t-test or Kruskal Wallis rank sum test, Pearson chi-squared test or the Fisher's exact test was performed as appropriate. The least absolute shrinkage and selection operator (LASSO) regression method was used for predictor selection and regularization. Multivariable logistic regression analysis using backward stepwise procedure and the likelihood ratio test were used to develop the predictive model. Nomogram was constructed to predict the diagnostic rate of PPLs with RP-EBUS-GS-TBLB. Model performance was assessed based on three dimensions: discrimination, calibration, and clinical usefulness. Discrimination was measured using the area under the curve (AUC) of the receiver operating characteristic (ROC) curve and internal validation was performed using bootstrapping (resampling = 500). Calibration was evaluated using calibration curves and unreliability tests. The clinical utility of the nomogram was assessed using decision curve analysis (DCA) by quantifying the standardized net benefit at different threshold probabilities. Statistical analysis was done using R software (version 4.2.1, http://www.r-project.org/), and P value < 0.05 was considered statistically signifcant.

Results

Baseline characteristics

We screened 242 hospitalized patients with PPLs primarily following RP-EBUS-GS-TBLB. 53 patients were excluded for the following reasons: 12 patients with serious complications during bronchsocopy; 31 patients combined use of other methods during bronchsocopy; 10 patients with insufficient information. The remaining 189 patients were collected. The flow chart shows the strategy to identify the participants with PPLs following RP-EBUS-GS-TBLB (Fig. 2). The demographic and clinical characteristics of patients diagnosed success (140/189) or failure (49/189) with RP-EBUS-GS-TBLB were summarized in Table 1. Table 1 showed that diagnostic success group had a significant difference with diagnostic failure group in terms of 8 factors, including lesion morphology in CT, distance from pleura, number of Biopsies, size, margin, shape, echogenicity and RP-EBUS location.

Independent risk factors in the cohort

From the 32 relevant feature variables, we selected 6 potential predictors with non-zero coefficients in the LASSO regression model (Fig. 3). These predictors include lesion morphology in CT, number of Biopsies, size, margin, echogenicity and RP-EBUS location.

Prediction model development

Following logistic regression analysis, the 6 predictors, lesion morphology in CT, number of Biopsies, size, margin, echogenicity and RP-EBUS location, all showed statistically significant differences. We applied EBUS imaging features (size, margin, echogenicity and RP-EBUS location; model 1) separately and combined them with clinical features (lesion morphology in CT and number of Biopsies; model 2) to develop two predictive models (Table 2). The nomogram was generated based on the contributed weights of factors (Predictive model 1: logit(diagnostic success) = − 11.22517 + 1.28881*size + 1.43183*margin + 3.29973*echogenicity + 1.07752*RP-EBUS location; Predictive model 2: logit(diagnostic success) =-14.28573 + 2.03989*lesion morphology(mixed) + 3.94300*lesion morphology(GG) + 1.47344*number of Biopsies + 1.39341*size + 1.73257*margin + 3.14848*echogenicity + 1.15015*RP-EBUS location) in the cohort to calculate the rate of diagnostic success (Fig. 4). In the nomogram, each factor has a related score for its contribution to diagnostic success.

Prediction model validation

For the prediction model, the area under the ROC curve for the model 1 was 0.901 (95% CI, 0.858–0.944), and it was 0.889 (95% CI, 0.826–0.943) in the internal validation using bootstrapping (resampling times = 500), indicating moderate performance (Fig. 5A and B). The area under the ROC curve for the model 2 was 0.927 (95% CI, 0.886–0.968), and it was 0.917 (95% CI, 0.862–0.959) in the internal validation using bootstrapping (resampling times = 500) (Fig. 6A and B), The calibration curves of the nomogram also showed good consistency (Fig. 7A and B). In conclusion, the nomogram of the model have good predictive ability. Decision curves (Fig. 8)

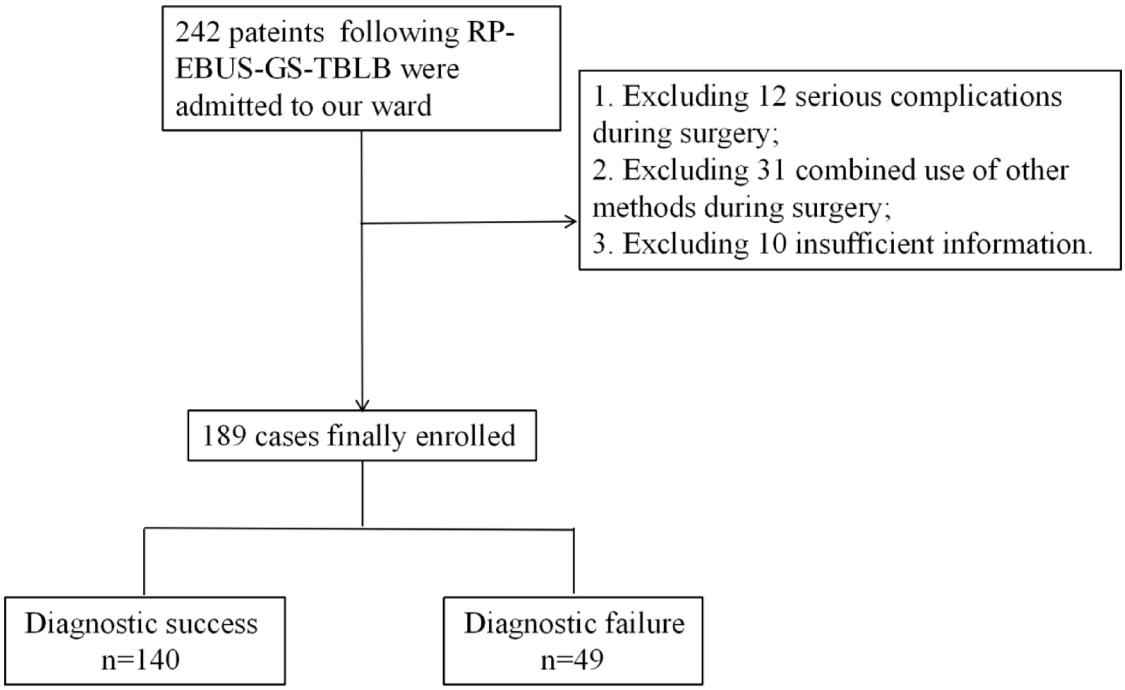

Fig. 2. Flow chart for patients screening.

Characteristic	Diagnostic success($n=140$)	Diagnostic failure($n=49$)	*P*
Age	57.70 ± 11.81	59.04 ± 10.46	0.481
Gender male	98 (70.00%)	30 (61.22%)	0.258
Smoking	47 (33.57%)	19 (38.78%)	0.511
Underlying lung disease			0.807
COPD	23 (16.43%)	7 (14.29%)	
Asthma	3 (2.14%)	2 (4.08%)	
ILD	5 (3.57%)	3 (6.12%)	
Other disease	13 (9.29%)	3 (6.12%)	
No	96 (68.57%)	34 (69.39%)	
Lesions location			0.098
Right upper lobe	20 (14.29%)	12 (24.49%)	
Right middle lobe	18 (12.86%)	3 (6.12%)	
Right lower lobe	33 (23.57%)	8 (16.33%)	
Left upper lobe	34 (24.29%)	18 (36.73%)	
Left lower lobe	35 (25.00%)	8 (16.33%)	
Lesion morphology			< 0.001
Solid	131 (93.57%)	33 (67.35%)	
Mixed	7 (5.00%)	9 (18.37%)	
Ground glass	2 (1.43%)	7 (14.29%)	
Distance from pleura	24.65 ± 11.81	19.96 ± 8.96	0.014
Anesthesia type (local)	112 (80.00%)	45 (91.84%)	0.057
Examination time (≥ 30 min)	66 (47.14%)	20 (40.82%)	0.444
Number of biopsies (≥ 5)	103 (73.57%)	20 (40.82%)	< 0.001
Size (≥ 2 cm)	62 (44.29%)	9 (18.37%)	0.001
Margin (distinct)	111 (79.29%)	23 (46.94%)	< 0.001
Shape (regular)	94 (67.14%)	22 (44.90%)	0.006
Echogenicity (homogeneous)	130 (92.86%)	18 (36.73%)	< 0.001
RP-EBUS location (within)	74 (52.86%)	12 (24.49%)	< 0.001

Table 1. Comparison of patients in diagnostic success and failure group.

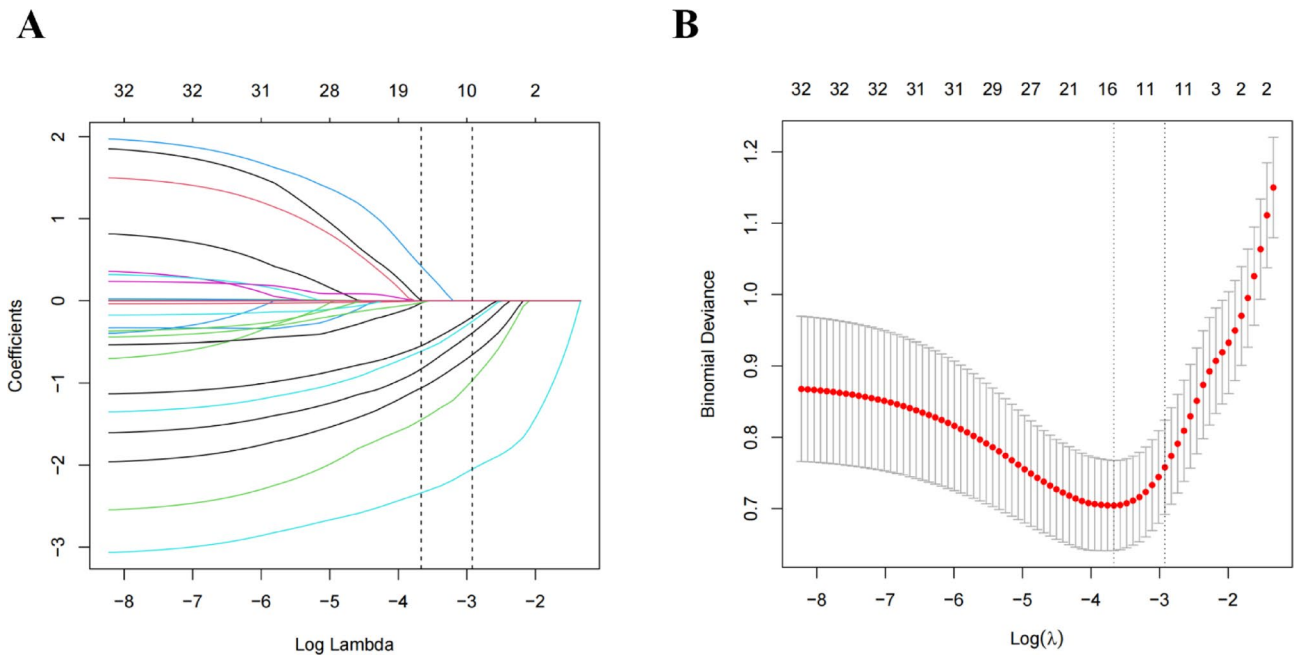

Fig. 3. Variable selection by LASSO binary logistic regression model. A coefficient profile plot was produced against the log(lambda) sequence (**A**). Six variables with nonzero coefficients were selected by optimal lambda. By verifying the optimal parameter (lambda) in the LASSO model, the partial likelihood deviance (binomial deviance) curve was plotted versus log(lambda) and dotted vertical lines were drawn based on 1 standard error criteria (**B**).

Independent variables	OR	95% CI	*P*
Model 1			
Intercept	0.02	0.00–0.06	< 0.001
Size (<2 cm)	3.63	1.28–10.30	0.015
Margin (indistinct)	4.19	1.68–10.46	0.002
Echogenicity (heterogeneous)	27.11	9.67–76.00	< 0.001
RP-EBUS location (adjacent)	2.94	1.12–7.72	0.029
Model 2			
Intercept	0.00	0.00-0.02	< 0.001
Lesion morphology (mixed)	7.69	1.83–32.37	0.010
Lesion morphology (GG)	51.57	3.41-779.72	0.004
Number of Biopsies (<5)	4.36	1.60-11.93	0.004
Size (<2 cm)	4.03	1.26–12.89	0.020
Margin (indistinct)	5.66	2.01–15.92	0.001
Echogenicity (heterogeneous)	23.30	7.21–75.28	< 0.001
RP-EBUS location (adjacent)	3.16	1.07–9.35	0.041

Table 2. Independent variables based on the Lasso-logistic regression in the cohort.

showed that the diagnostic rate with RP-EBUS-GS-TBLB were more accurately predicted using these nomogram. We also compared the AUC of two models (Fig. 9A and B), However, there is no significant difference in AUC between the two models both in training($P = 0.109$) and internal validation($P = 0.203$).

Discussion

This study investigated factors contributing to the diagnostic rate of RP-EBUS-GS-TBLB in PPLs. The findings identified lesion morphology in CT, number of Biopsies, size, margin, echogenicity and RP-EBUS location as independent risk factors. Using these risk factors, we developed two prediction model, which demonstrated strong predictive accuracy, discrimination, and clinical utility. We also compared the AUC of two models, the results indicated that the model only using EBUS imaging features can serve as a concise and efficient predictive model.

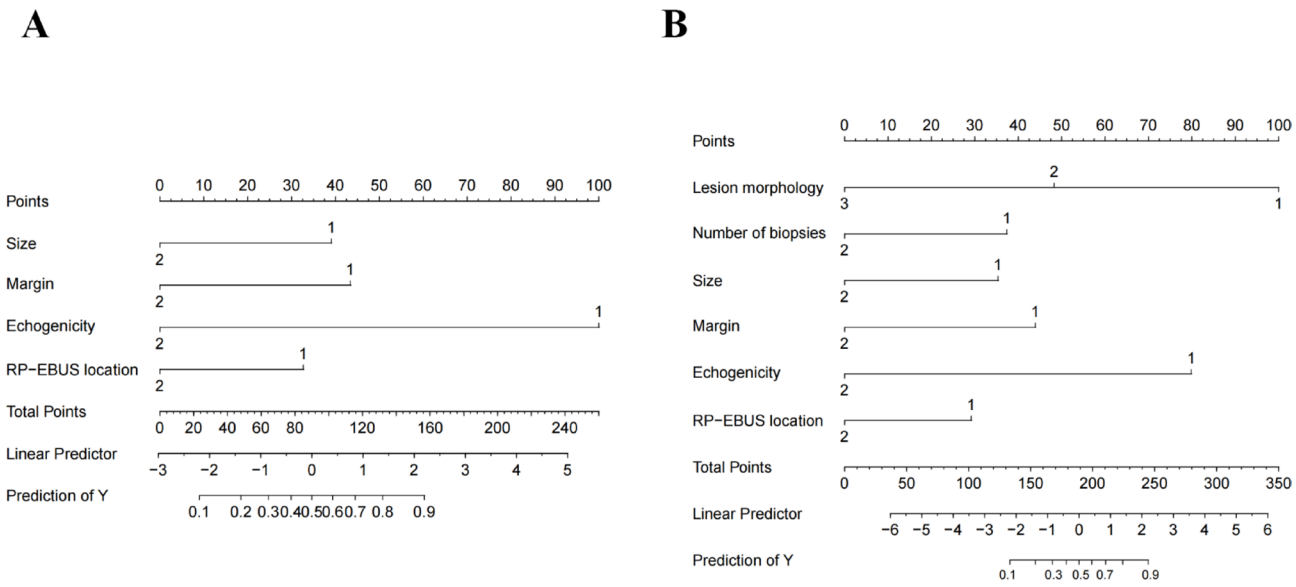

Fig. 4. The nomogram for predicting diagnostic rate of RP-EBUS-GS-TBLB in PPLs based on the Lasso-logistic regression. (**A**) Nomogram for model 1 (Size 1 ≥ 2 cm, 2 <2 cm; Margin 1 distinct, 2 indistinct; Echogenicity 1 homogeneous, 2 heterogeneous; RP-EBUS location 1 within, 2 adjacent). (**B**) Nomogram for model 1 (lesion morphology 1 solid, 2 mixed, 3 GG; Number of Biopsies 1 ≥ 5, 2 <5).

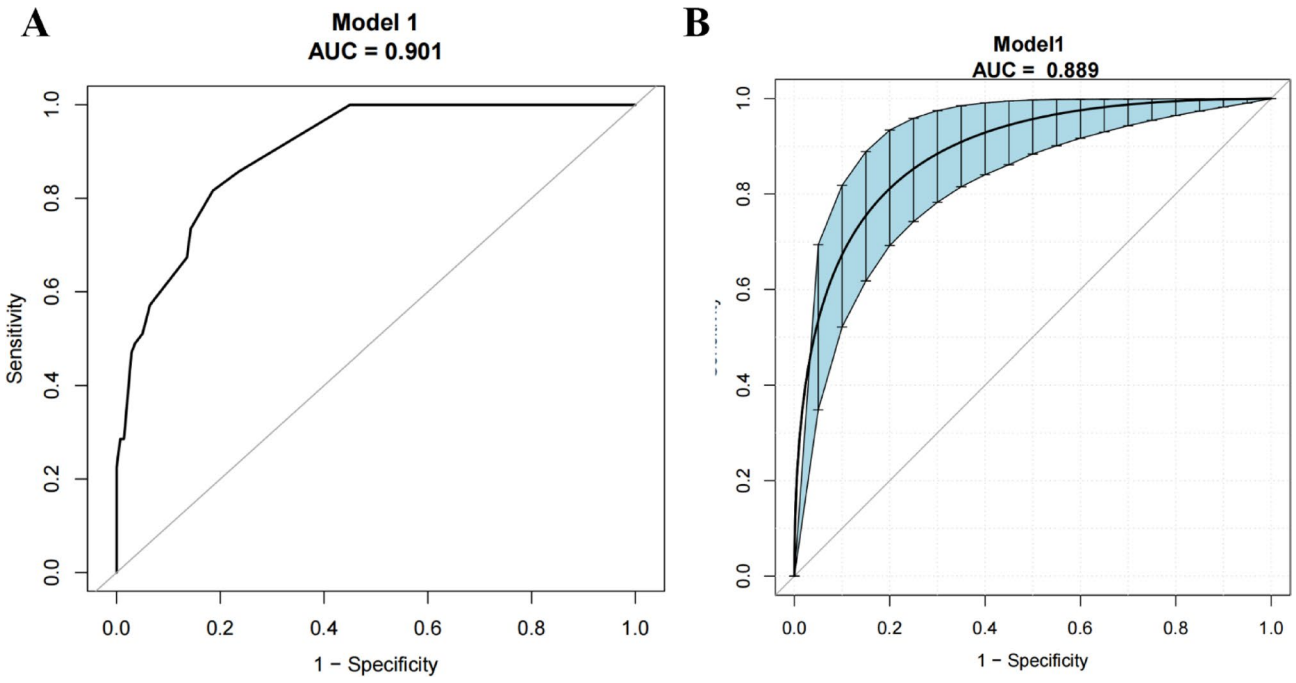

Fig. 5. ROC validation of the model 1 prediction of the diagnostic rate of RP-EBUS-GS-TBLB in PPLs. The y-axis represents the rate of true positives for the risk prediction. The x-axis represents false positives for the risk prediction. The area under the curve represents the performance rate of the nomogram. (**A**) Shows AUC of the predictive model and (**B**) shows AUC of the internal validation with the bootstrap method (resampling times = 500). The dotted vertical lines represent 95% confidence interval.

Performance of routine bronchoscopy (without r - ebus or fluoroscopy) is known to be not ideal in assessment of peripheral pulmonary lesions, for adjacent bronchus is relatively narrow for the endoscope to pass. With the development of high-frequency radial ultrasonic probe, EBUS can clearly show the distal lesions outside the lumen. RP-EBUS-GS-TBLB was the main method in the assessment of PPLs[10–12].

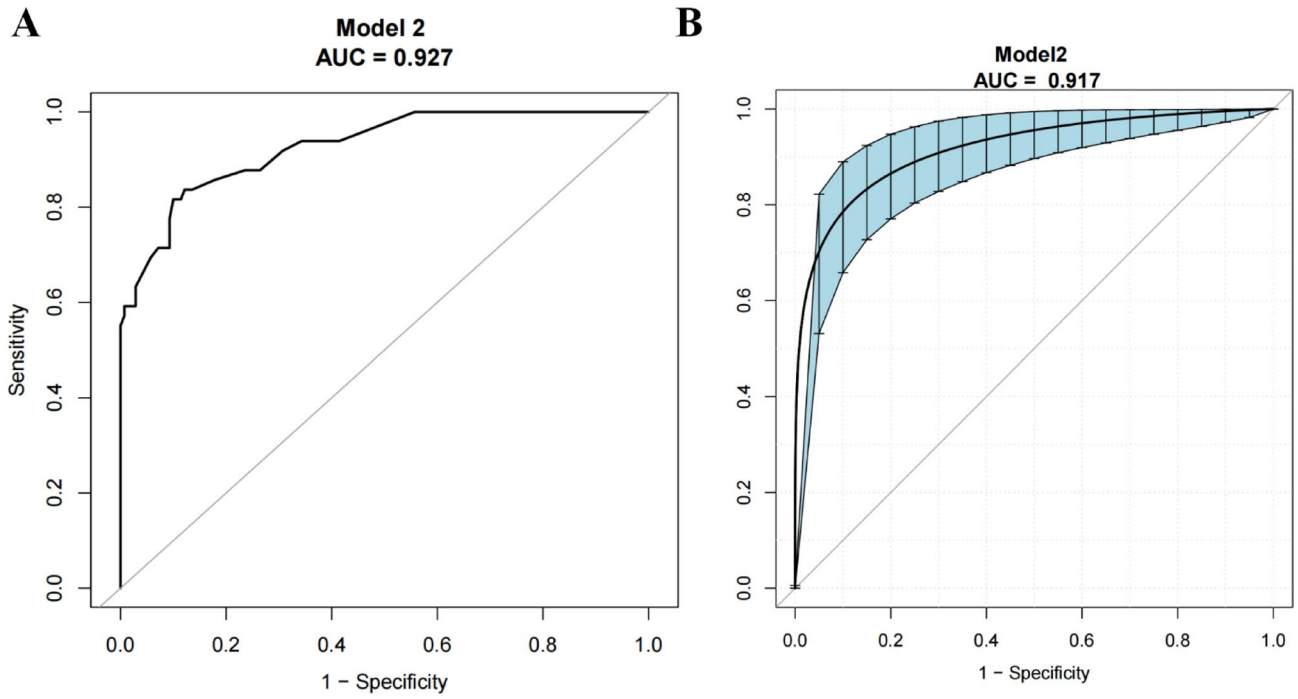

Fig. 6. ROC validation of the model 2 prediction of the diagnostic rate of RP-EBUS-GS-TBLB in PPLs. (**A**) shows AUC of the predictive model and (**B**) shows AUC of the internal validation with the bootstrap method (resampling times = 500). The dotted vertical lines represent 95% confidence interval.

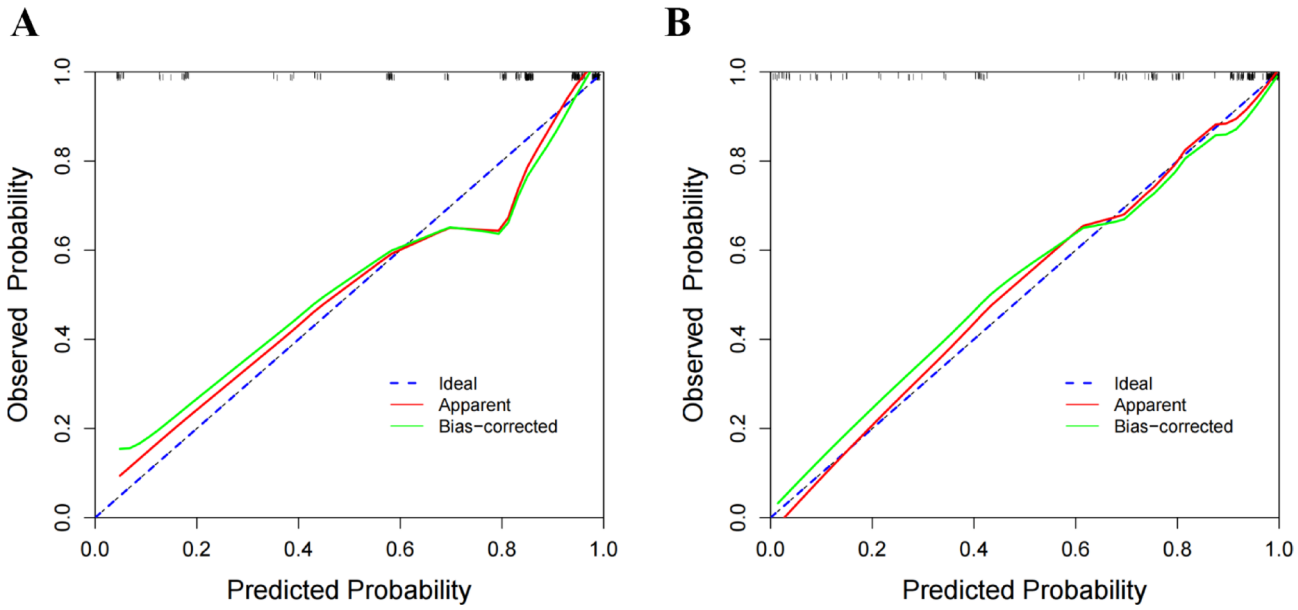

Fig. 7. Calibration curves of the risk nomogram prediction of the diagnostic rate of RP-EBUS-GS-TBLB in PPLs. The y-axis meant the actual diagnostic success. The x-axis meant the predicted diagnostic success. The blue line represents an ideal predictive model, and the solid red line shows the actual performance of the model 1 (**A**) and model 2 (**B**). The green line represents a bias-corrected performance.

In this study, we employed Lasso-logistic regression modeling, which allowed for the integration of multiple potential risk factors into a single predictive tool, providing greater prognostic accuracy. Six significant risk factors, including lesion morphology in CT, number of Biopsies, size, margin, echogenicity and RP-EBUS location were identified as predictors. Our study found that the overall incidence for diagnostic rate of RP-EBUS-GS-TBLB in PPLs was 74.07%. This result was similar to other studies[16]. Based on these findings, we developed and validated a new predictive tool using these key variables.

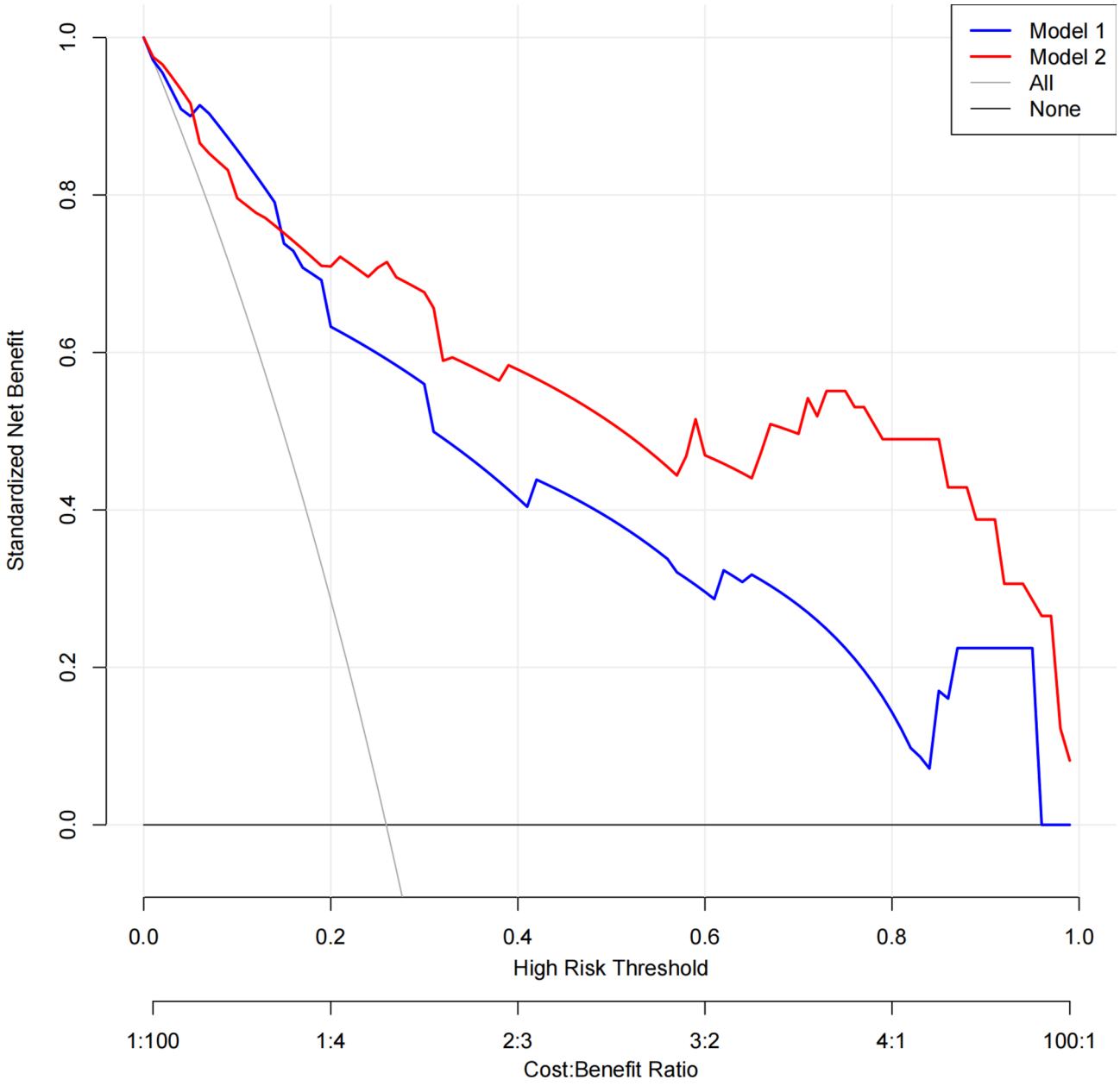

Fig. 8. Decision curve of two predictive model. Net benefit was produced against the high risk threshold.

In this study, we firstly applied EBUS imaging features to develop a predictive model. In this model, EBUS imaging features including size, margin, echogenicity and RP-EBUS location were identified as significant risk factors, with positive correlation between bigger size(≥ 2 cm OR = 3.63, 95% CI 1.28–10.30), distinct margin(OR = 4.19, 95% CI 1.68–10.46), homogeneous echogenicity(OR = 27.11, 95% CI 9.67–76.00), radial probe within the lesion(OR = 2.94, 95% CI 1.12–7.72) and increased diagnostic rate. The mechanism may involve that: 1. With the patient's breathing or coughing, GS will move slightly, so the larger the lesion, the less impact it has on sampling; 2. The regularity and eccentricity of the lesion shape indicate the degree of invasion of the trachea by the lesion, which is important to successful sampling[13,14]; 3. The heterogeneous echogenicity may represent the degree of necrosis of the lesion, which determines whether enough tissue specimens can be obtained.

In addition, we also applied EBUS imaging features and lesion morphology in CT, number of Biopsies to develop another predictive model. In this model, lesion morphology in CT, number of Biopsies were identified as significant risk factors, with positive correlation between more Biopsies(≥ 5 OR = 4.36, 95% CI 1.60–11.93), solid lesion in CT and increased diagnostic rate. The mechanism may involve that solid lesions are more likely to invade the airway than mixed or ground glass lesions[15].

Additionally, both the two prediction model showed good discrimination ability and calibration. The decision curve based on this model revealed that the model to predict diagnostic rate would benefit when compared to either treat-all or treat-none strategies. In addition, the nomogram was also constructed to facilitate the

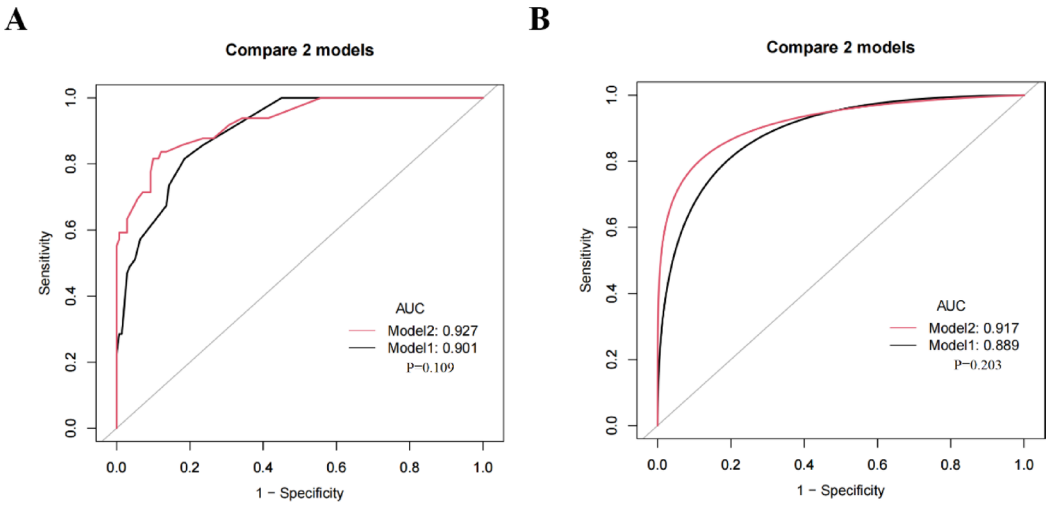

Fig. 9. comparison of ROC validation of two models. (**A**) shows AUC of the predictive model and (**B**) shows AUC of the internal validation with the bootstrap method (resampling times = 500).

application of the model. We also compared the AUC of two models, However, there is no significant difference in AUC between the two models both in training and internal validation, which suggest that the model 1(only using EBUS imaging features) can serve as a concise and efficient predictive model.

Previous studies have constructed predictive models based on r-ebus imaging features to differentiate benign and malignant peripheral pulmonary lesions and achieved good results. It found significant differences in size, shape, margin, and other features between benign and malignant lesions. A sum score model based on these features achieved a diagnostic accuracy of 79.54% in the model group and 82.76% in the verification group, indicating its potential diagnostic value[16]. In our study, we constructed a model based on r - ebus imaging features and further compared it with the traditional clinical feature model, clarifying the advantage of the imaging predictive model in the diagnostic rate of peripheral pulmonary diseases.

This study also has several limitations. Firstly, these models was constructed based on a singlecenter retrospective study, which inevitably suffered from confounding bias;. Secondly, an independent validation is very important for determining the clinical usefulness of a predictive model; therefore, whether the proposed model is applicable to other endoscopic centers needs further validation. Future studies should involve larger sample sizes, multicenter prospective studies, or randomized controlled trials (RCTs) incorporating advanced algorithms, such as machine learning, to further validate our findings. In addition, In peripheral pulmonary nodules, the diagnosis of the nature of the nodule, especially the differentiation between benign and malignant lesions, is a very important part. Our current predictive model focuses on the probability of successful diagnosis. In future applications, the model can be applied to the differentiation between benign and malignant lesions for further testing, providing more application scenarios for the model.

Conclusion

In this study, we analyzed the risk factors that may contribute to the diagnostic rate of RP-EBUS-GS-TBLB in PPLs. Six factors were identified as significant risk contributors: lesion morphology in CT, number of Biopsies, size, margin, echogenicity and RP-EBUS location. Based on these findings, we developed and compared two models to predict the diagnostic rate of RP-EBUS-GS-TBLB in PPL. Finally we chose the model only using EBUS imaging features as the concise and efficient predictive model. The nomogram demonstrated strong predictive accuracy, discriminative power, and clinical utility in both the training and validation sets, indicating its potential effectiveness in practical applications.

Data availability

The original contributions presented in the study are included in the article. Further inquiries can be directed to the corresponding author.

Received: 29 November 2024; Accepted: 20 October 2025
Published online: 21 November 2025

References

1. Lee, J. & Song, J. U. Diagnostic yield of radial probe endobronchial ultrasonography-guided transbronchial biopsy without fluoroscopy in peripheral pulmonary lesions: a systematic review and meta-analysis. *Thorac. Cancer.* **14** (2), 195–205 (2023).
2. Lee, Y. S. et al. Efficacy and safety of radial probe endobronchial ultrasound-guided biopsy for peripheral lung lesions in chronic obstructive pulmonary disease patients. *Transl. Lung Cancer Res.* **13** (10), 2500–2510 (2024).
3. Yuan, M. et al. Diagnostic outcomes of radial endobronchial ultrasound bronchoscopy guided by manual navigation in the evaluation of peripheral pulmonary lesions: an observational study. *Clin. Respir J.* **18** (5), e13768 (2024).

4. Balasubramanian, P. et al. Diagnostic yield and safety of diagnostic techniques for pulmonary lesions: systematic review, meta-analysis and network meta-analysis. *Eur. Respir Rev.*, **33**(173), 240046 (2024).
5. Sryma, P. B. et al. Efficacy of radial endobronchial ultrasound (R-EBUS) guided transbronchial cryobiopsy for peripheral pulmonary lesions (PPL… s): a systematic review and meta-analysis. *Pulmonology* **29** (1), 50–64 (2023).
6. Zhan, P. et al. Comparison between endobronchial ultrasound-guided transbronchial biopsy and CT-guided transthoracic lung biopsy for the diagnosis of peripheral lung cancer: a systematic review and meta-analysis. *Transl. Lung Cancer Res.* **6** (1), 23–34 (2017).
7. Kim, S. H. et al. Development of the Korean association for lung cancer clinical practice guidelines: recommendations on radial probe endobronchial ultrasound for diagnosing lung cancer—an updated meta-analysis. *Cancer Res. Treat.* **56** (2), 464–483 (2024).
8. Ali, M. S. et al. Radial endobronchial ultrasound for the diagnosis of peripheral pulmonary lesions: a systematic review and meta-analysis. *Respirology* **22** (3), 443–453 (2017).
9. Steinfort, D. P. et al. Radial probe endobronchial ultrasound for the diagnosis of peripheral lung cancer: systematic review and meta-analysis. *Eur. Respir J.* **37** (4), 902–910 (2011).
10. Wang, W. et al. Evaluation of the diagnostic role of radial probe endobronchial ultrasound for peripheral pulmonary lesions. *Clin. Respir J.* **18** (7), e13792 (2024).
11. Xie, Q. et al. Improved diagnostic yield of peripheral pulmonary malignant lesions with emphysema using a combination of radial endobronchial ultrasonography and rapid on-site evaluation. *BMC Pulm Med.* **24** (1), 401 (2024).
12. Tian, S. et al. Radial endobronchial ultrasound—guided bronchoscopy for the diagnosis of peripheral pulmonary lesions: a systematic review and meta-analysis of prospective trials. *Heliyon* **10** (8), e29446 (2024).
13. Moulton, N. et al. Inter- and intra-observer variability of radial-endobronchial ultrasound image interpretation for peripheral pulmonary lesions. *J. Thorac. Dis.* **16** (1), 450–456 (2024).
14. Yamamoto, S. et al. Predictors of improvement of radial-endobronchial ultrasonography findings from adjacent to to within in endobronchial ultrasonography using a guide sheath: a retrospective cohort study. *J. Thorac. Dis.* **16** (1), 264–272 (2024).
15. Park, J. et al. Endobronchial ultrasound using guide Sheath-Guided transbronchial lung biopsy in Ground-Glass opacity pulmonary lesions without fluoroscopic guidance. *Cancers (Basel).* **16**(6), 1203 (2024).
16. Zheng, X. et al. Diagnostic value of radial endobronchial ultrasonographic features in predominant solid peripheral pulmonary lesions. *J. Thorac. Dis.* **12** (12), 7656–7665 (2020).

Author contributions
ML Z and YH G were involved in the design of the study protocol, data collection, and follow-up; ML Z and CP Y were involved in the analysis of the data and the production of the pictures and tables; ML Z completed the manuscript. All authors reviewed and edited the manuscript. All authors have read and agreed to the final version of the manuscript.

Funding
This article was funded by Capital's Funds for Health Improvement and Research (No.2024-2-5091); Beijing Key Laboratory Opening Fund (No. BJZDSYS-2022-3). PLA General Hospital New Technology Project.

Declarations

Competing interests
The authors declare no competing interests.

Ethical approval
All procedures performed in studies involving human participants were in accordance with the ethical standards of the institutional and/or national research committee and with the 1964 Helsinki Declaration and its later amendments or comparable ethical standards. This study was approved by the institutional ethics committee of the hospital (The Ethics Committee of 8th Medical Centre, Chinese PLA General Hospital, Beijing, China No. 202400216). Written informed consent was obtained from all participants before inclusion.

Consent for publication
Not applicable.

Additional information
Correspondence and requests for materials should be addressed to M.Z. or Y.G.

Reprints and permissions information is available at www.nature.com/reprints.

Publisher's Note Springer Nature remains neutral with regard to jurisdictional claims in published maps and institutional affiliations.